Struct Bond (2014) 158: 161–190
DOI: 10.1007/430_2013_91
© Springer-Verlag Berlin Heidelberg 2013
Published online: 19 April 2013

Crystallization and Dissolution in Aqueous Solution: A Bond-Valence Approach

Frank C. Hawthorne and Michael Schindler

Abstract In many groups of minerals, structural diversity occurs by polymerization of a small number of clusters (or fundamental building blocks). Where these minerals crystallize from aqueous or hydrothermal solutions, the fundamental building blocks occur as aqueous species in solution, and it seems reasonable to conclude that crystallization of these minerals occurs by condensation of these clusters in solution. The variation in Lewis acidity of these clusters is a function of the pH of the aqueous solution in which they occur, in accord with the different structures crystallizing from similar aqueous solutions at different pH. Strongly bonded polyhedron chains (equivalent to periodic bond-chains) control the morphology of crystals. Anions at the surface of a mineral (i.e., exposed to an ambient aqueous solution) are called *terminations*, and the residual valence at a termination controls its reactivity (i.e., is the driving force for reaction with the aqueous solution). The residual valence of a polyhedron chain controls the growth or dissolution rate at the crystal face associated with that chain and may be calculated as the net residual valence of the terminations per repeat of the polyhedron chain. Edges involving polyhedron chains with low normalized residual valence will grow slowly, whereas edges involving polyhedron chains with high normalized residual valence will grow rapidly, and the relative morphology of crystals will be controlled by the relative magnitudes of the residual valence of polyhedron chains parallel to specific faces. The observed morphology of selected uranyl-oxide hydroxyl-hydrate and borate minerals is in reasonable accord with this approach.

Keywords Aqueous speciation · Bond valence · Borate minerals · Crystallization · Dissolution · Morphology · Surface structure · Uranyl minerals

F.C. Hawthorne (✉)
Department of Geological Sciences, University of Manitoba, Winnipeg, MB, Canada R3T 2N2
e-mail: frank_hawthorne@umanitob.ca

M. Schindler
Department of Earth Sciences, Laurentian University, Sudbury, ON, Canada P3E 2C6

Contents

1 Introduction 162
1.1 Aqueous Solutions 163
1.2 The Effect of pH on Aqueous Complexes and Crystal Structure 165
2 Crystal Faces 166
3 Interaction of a Surface with an Aqueous Solution: A Bond-Valence Perspective 166
4 Surface Features on Crystal Faces 168
4.1 Residual Valence at an Anion Termination and at a Surface Polyhedron Chain ... 169
4.2 Point of Zero Charge and Net Proton Charge: A Bond-Valence Perspective 170
5 Application to Minerals 171
5.1 Uranyl Minerals 172
5.2 Borate Minerals 176
6 Crystallization and Dissolution 178
6.1 Uranyl Minerals 178
6.2 Borate Minerals 180
7 Quantitative Aspects of Crystallization and Dissolution 181
7.1 Residual Valence, Kink Sites, and O^{2-} Ligands 181
7.2 Uranyl Minerals 182
7.3 Borate Minerals 184
8 Summary 186
References 187

Abbreviation

v.u Valence units

1 Introduction

A basic axiom of bond-valence theory is the valence-sum rule [1]: *The sum of the bond valences at each atom is equal to the magnitude of the atomic valence.* This rule has been shown to hold (within a few percent) for a large number of crystal structures. For most of the structures in which we are interested (minerals), the maximum valences of the cations (4^+ to 6^+) generally exceed the maximum valences of the anions (2^-). The result is that we can identify strongly bonded oxyanions, e.g., $(SiO_4)^{4-}$, $(PO_4)^{3-}$, $(SO_4)^{2-}$, in these structures, and it is these oxyanions that dominate their structural characteristics and geochemical behavior [2, 3]. A primary interest in mineralogy is the behavior of minerals in geological processes, in particular crystallization and dissolution, as the structural and chemical characteristics of minerals can carry a lot of information on the conditions under which they form. Hence a mechanistic understanding of the processes of crystallization and dissolution of minerals is of considerable interest. Many minerals crystallize from aqueous solution or magma, both of which have some regularity

in their structure (i.e., a nonrandom arrangement of their constituent atoms). Hawthorne [4] proposed the *reaction principle*: *During a chemical reaction, atoms move relative to each other such that they continually minimize local deviations from the valence-sum rule.* This rule implies that the atomic arrangements in the reactants affect the atomic arrangements in the products of any chemical reaction. If this is the case in geological processes, we need to focus not just only on the atomic arrangements in the resulting minerals but also on the atomic arrangements in the precursor phases, i.e., aqueous solutions and magmas, and the atomic arrangements of any intermediate phases, e.g., the interfaces between the reactant phase(s) and the product phase(s).

1.1 Aqueous Solutions

1.1.1 Borates

Hawthorne [5–7] showed that structural diversity in oxysalt minerals (specifically phosphates) occurs by polymerization of a small number of clusters (fundamental building blocks) to form chains, sheets, and frameworks and suggested that structural units in many low-temperature minerals form by condensation of fundamental building blocks that occur as aqueous complexes in hydrothermal or aqueous solutions. With regard to borates, Ingri and coworkers (reviewed in [8]) showed that the following borate species occur in highly concentrated aqueous borate solutions with decreasing pH: $[B(OH)_3]^0$, $[B_5O_6(OH)_4]^-$, $[B_3O_3(OH)_4]^-$, $[B_3O_3(OH)_5]^{2-}$, $[B_4O_5(OH)_4]^{2-}$ and $[B(OH)_4]^-$ and noted that "polyanions of the kind found in crystals exist in solution.....and are readily available for the building of crystals." Furthermore, ^{11}B-NMR spectroscopy [9–11] and Raman spectroscopy [12, 13] have confirmed the occurrence of all these aqueous species except $[B_3O_3(OH)_5]^2$. With regard to borate minerals, Christ et al. [14] used the data summarized in [8] to illustrate the variation in aqueous borate species and their variation in abundance in solution as a function of pH (Fig. 1). $[B(OH)_3]^0$ is the stable species at low pH and $[B(OH)_4]^-$ is the stable species at high pH, while around a pH of 8, the more complicated species $[B_5O_6(OH)_4]^-$, $[B_3O_3(OH)_4]^-$, $[B_3O_3(OH)_5]^2$, and $[B_4O_5(OH)_4]^{2-}$ occur in solution and show their maximum concentrations at slightly different values of pH. From Fig. 1, Schindler and Hawthorne [2, 15] calculated the percentage of $^{[4]}$B in aqueous solution and showed that it is a smooth function of pH (Fig. 2). This suggests that the stability (i.e., existence) of each cluster and the relative amounts of each cluster as a function of pH are controlled by bond-valence matching between the clusters and their host aqueous solution.

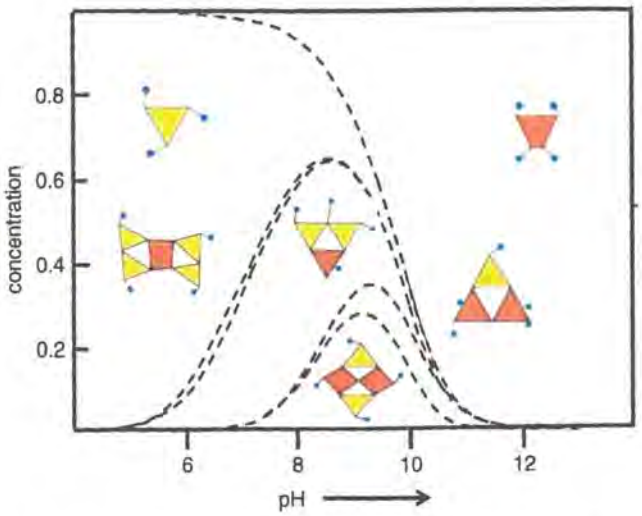

Fig. 1 The distribution of B species in aqueous solution of 0.40 M on total $B(OH)_3$; ($B\varphi_3$): *yellow/pale-gray*; ($B\varphi_4$): *orange/medium-gray*; after [14] from the data of [8]

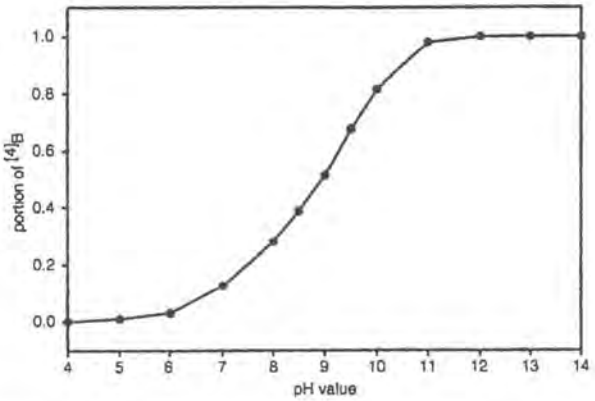

Fig. 2 The fraction of $^{[4]}B$ in the aqueous species in solution as a function of pH in the aqueous solution shown in Fig. 1

1.1.2 Uranyl Oxide-Hydroxy-Hydrates

The hydrolysis of dioxouranium(VI) can be formulated as follows:

$$m{UO_2}^{2+} + nH_2O(l) \rightarrow (UO_2)_m(OH)_{2m-n}$$

Grenthe et al. [16] reviewed the thermodynamic data for $(UO_2)_m(OH)_{2m-n}$ species and listed eighteen different species. However, spectroscopic evidence exists only for a few species, and Grenthe et al. [16] indicated that the thermodynamic data for some of these 18 species are questionable. Tsushima et al. [17]

showed by EXAFS, FTIR, and UV–vis spectroscopy and DFT calculations that in aqueous solution, $(U^{6+}O_2)^{2+}$ always has five peripheral anions, the monomer, dimer and trimer are present, and there is edge-sharing between uranyl polyhedra. Although we do not know the exact distribution of all $(UO_2)_m(OH)_{2m-n}$ species as a function of pH, the information given in [17] is sufficient to allow us to consider crystallization and dissolution mechanisms for uranyl-oxide hydroxyl-hydrate minerals.

1.2 *The Effect of pH on Aqueous Complexes and Crystal Structure*

1.2.1 Borates

The relative amount of $^{[4]}B$ in solution is a function of the pH of that solution, and it seems reasonable to propose that aqueous borate complexes adjust to varying pH by varying the relative amounts of $^{[3]}B$ and $^{[4]}B$. In the crystal structures of the sedimentary borate minerals, these clusters in aqueous solution are the fundamental building blocks of all the borate minerals [18]. This implies that the structural units in borate minerals form by condensation of these complexes in hydrothermal or aqueous solutions, and their relation with pH gives us a direct relation between the pH of the nascent solution and the chemical compositions and structures of the crystallizing minerals.

1.2.2 Uranyl Oxide-Hydroxy-Hydrates

The situation for the uranyl oxide-hydroxy-hydrates is somewhat different from that of the borate minerals. The coordination number of U^{6+} does not change as a function of pH; it is [7] across the whole range. What will change as a function of pH is the polymerization and the ligancy in the clusters. If minerals form by condensation of these complexes in aqueous solution, the pH at which they crystallize should relate to the stability of the clusters that constitute the fundamental building blocks of the structure. There is general consensus on the occurrence of the aqueous species $(UO_2)^{2+}$ and $(UO_2)_3(OH)_5^+$, which occur in strongly and weakly acidic to neutral aqueous solutions, respectively [19]. Schoepite, $(UO_2)_8O(OH)_{12}(H_2O)_{12}$, is a uranyl-oxide hydroxy-hydrate mineral which contains sheets of polymerized trimers and dimers of (edge-sharing) $(U^{6+}O_2\varphi_5)$ polyhedra [φ = (OH), (H_2O)]. Schindler and Putnis [20] synthesized well-crystaline schoepite under weakly acidic conditions (pH = 5.5–6.5) which overlap with the general occurrence of the $(UO_2)_3(OH)_5^+$ species in solution, suggesting that the crystallization of schoepite is controlled by the polymerization of aqueous species present in solution (see below).

2 Crystal Faces

Hartman and Perdok [21–23] proposed that where an atom or cluster of atoms attaches to a growing surface of a crystal, the probability of subsequent detachment is inversely proportional to the number of strong bonds between the atom or cluster and the crystal surface. The focus is on uninterrupted chains of strong bonds between building units, called periodic bond-chains. Periodic bond-chains define the major growth direction(s) of a crystal. There are three types of faces: F (or flat) faces with two or more types of periodic bond-chains parallel to the face; S (or stepped) faces with one type of periodic bond-chain parallel to the face, and K (or kinked) faces with no periodic bond-chains parallel to the face. The morphology of a crystal is controlled primarily by the occurrence of F faces and secondarily by the occurrence of S faces. Complicated oxide and oxysalt structures are generally represented as arrangements of polyhedra, where each polyhedron consists of a central cation and its coordinating anions. This type of representation leads to major simplification in representing and understanding the topological aspects of the arrangements of chemical bonds, and the linkage of such polyhedra is used as a basis for hierarchical classification of crystal structures (e.g., [18, 24–26]). We will follow this polyhedron approach in considering surfaces of crystals and will consider periodic bond-chains as *polyhedron chains.*

Molecular modeling may be used to examine the morphology of crystals by calculating surface energies or step energies, provided good interaction potentials are available for the constituent species. This is usually not the case for hydroxy-hydrated oxysalt minerals which contain unusual coordination geometries and both (OH) and (H_2O) groups, e.g., althupite, $AlTh[(UO_2)\{(UO_2)_3(PO_4)_2(OH)O\}_2](OH)_3(H_2O)_{15}$. As many such minerals are important phases from an environmental perspective, and such minerals constitute the bulk of the mineral kingdom, we need an approach that is tractable for such complicated materials. Bond-valence theory is a key part of such an approach.

3 Interaction of a Surface with an Aqueous Solution: A Bond-Valence Perspective

The valence-sum rule (Eq. 2 in chapter "Bond Valence Theory") requires that the sum of the bond-valences incident at any cation or anion must be equal to its valence. It is useful to regard bond valences as directed, as this keeps track automatically of the nature (cation or anion) of the ion occupying any site in a structure. Here, we adhere to the convention that bond valences from a cation to an anion are positive, and bond valences from an anion to a cation are negative.

For a surface, we may identify two situations: (1) the surface of the crystal is adjacent to a vacuum and (2) the surface of the crystal is adjacent to a liquid (or gas). In the first situation, the surface ions must have coordinations different from those in

the bulk crystal, and the surface structure responds to these differences by lengthening or shortening specific bonds (relaxation), and there may be a reorganization of the topology of the chemical bonds at the surface (cf. in Chapter "Structure and Acidity in Aqueous Solutions and Oxide–Water Interfaces"). In the second situation, the bond-valence requirements of the surface atoms are partly met by adjacent atoms in the coexisting liquid (or gas), and surface relaxation will be much less than where the surface is exposed to a vacuum. For a crystal surface in equilibrium with an aqueous solution, the surface is partly or fully hydrated, depending on the pH of the solution, and aqueous species in the solution bond to anions or cations on the surface. The type of anion or cation on the surface and the conditions in the coexisting solution will affect the degree of hydration and type of attachment. The atoms of the liquid will tend to arrange themselves such that surface relaxation is minimized, and one may well be able to consider local atom interactions as the average of what occurs at the surface over a longer timescale. In turn, this suggests that we may be able to approximate bond valences of near-surface bonds as equal to the bond valences of the analogous bonds in the bulk structure.

The conditions in the coexisting aqueous solution and the anions or cations at the surface will affect the degree of hydration and the type of reactions that can occur at the surface. The degree of hydration will be a function of the bond-valence requirements of the anions at the surface and the pH of the solution. The bond-valence requirements of the surface anions can be predicted using the MUSIC ("MUltiSIte Complexation") model of Hiemstra et al. [27] using the equation

$$pK_a = -A\left(\sum s_j + V\right) \tag{1}$$

where pK_a is the intrinsic acidity constant, A equals 19.8, V is the valence of the surface O atom (−2), and $\sum s_j$ is the bond-valence sum at the surface O atom and is defined as

$$\sum s_j = \{s_M + ms_H + n(1 - s_H)\} \tag{2}$$

where s_M is the valence of the M–O bond, s_H is the bond valence of the H–O bond to the surface oxygen if the base is an (OH) group (assumed to be 0.80 v.u. [1]), $(1 - s_H)$ is the valence of weak hydrogen bonds from aqueous species to surface anions, and m and n are the numbers of stronger O–H and weaker O···H bonds, respectively. Hiemstra et al. [27] used bond valences from unrelaxed bulk structures. Conversely, for the calculation of intrinsic pK_a values, Bickmore et al. [28, 29] considered unevenly distributed charge densities and relaxed metal–oxygen bonds on surfaces.

The intrinsic acidity constant is a measure of the strength of an acid (HA) in an acid–base equation, $HA + H_2O \leftrightarrow A^- + H_3O^+$, and is closely related to the ability of the conjunctive base (H_2O is a Lewis base) to donate electrons to the acid (H^+,

Lewis acid). Schindler and Hawthorne [30] defined the Lewis base-strength of a complex structural unit as the bond valence required by the (negatively charged) structural unit divided by the number of (weak) bonds accepted by the structural unit from the interstitial complex. Using this definition, we may calculate the Lewis base strength (or Lewis acid strength) of arrangements of atoms at a surface. A key issue in the calculation of intrinsic acidity constants and Lewis basicities is use of the correct average coordination number of O at the surface. Hiemstra et al. [27] used an average O-coordination of [3] for the surfaces of gibbsite and goethite and an average O-coordination number of [4] for the surface of quartz. The resulting intrinsic acidity constants were used to calculate the point of zero charge for gibbsite, goethite, and quartz and the results agree with experimental values. Schindler et al. [31] used an average O-coordination of [4] for the surfaces of uranyl-oxide and oxysalt structures, and the resulting Lewis basicities of the various arrangements of surface atoms are strongly correlated with the measured pK_a values.

4 Surface Features on Crystal Faces

A strongly bonded polyhedron chain which occurs on a crystal face contains ligands which bond either to cations of the chain or both to cations of the chain *and* to species in the adjacent aqueous solution. Any anion on such a chain and the cations to which it is bonded form a *termination*. Polyhedron chains are generally linear and have a small number of cation–φ (anion) terminations per unit length. In general, it is the incident bond-valence at the anion of the (bare) termination that controls the reactivity of that termination. If the incident bond-valence at the anion already satisfies the valence-sum rule, $pK_a = 0$ in Eq. (1) and there is no driving force for that anion to react with any component of the adjacent aqueous solution. Conversely, if the incident bond-valence at the anion is less than that required by the valence-sum rule, the anion will react with some component of the adjacent aqueous solution to accord with the valence-sum rule.

Crystal faces invariably have surface features that are due to addition or removal of atoms during crystallization or dissolution. Addition of one or more layers of structure can form surface features such as *terraces* and *steps* on a face. The termination of one structural unit orthogonal to a face is called an *edge* (Fig. 3). Termination of an edge forms a *kink* site, where a strongly bonded polyhedron chain ends. An array of coplanar edges defines a *step* or a *face* non-coplanar with the original face. Similarly, removal of atoms often gives rise to depressions or etch pits whose boundaries are crystallographically controlled. The atomic environment at an edge or step will strongly affect the local reactivity between the surface and an adjacent aqueous solution, and this reactivity will vary also as a function of the pH of the solution.

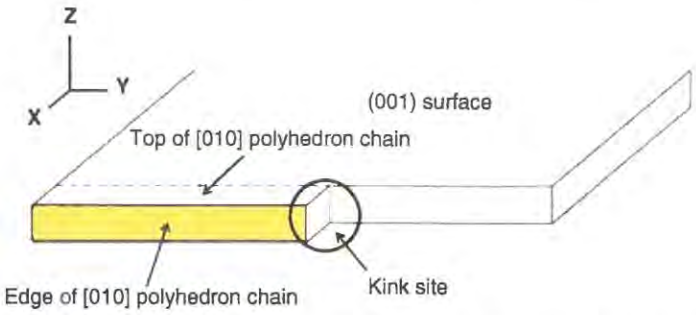

Fig. 3 Sketch of a (0 0 1) surface of a crystal with a [0 1 0] polyhedron forming an edge (*shaded*) and a kink site on the surface; the orientation of these features is the same as those in Figs. 8 and 9

4.1 *Residual Valence at an Anion Termination and at a Surface Polyhedron Chain*

We need to know the residual valence at an anion termination in order to calculate the intrinsic acidity constant and the Lewis basicity of that anion termination, as the mean coordination number of the O-atom at an anion termination scales the absolute values of the intrinsic acidity constant and the Lewis basicity. The residual valence at an O-atom, Δs ($=\sum s_j + V$), can be related to the free energy of any acid–base reaction in which it is involved [32]:

$$\Delta_R G_{AT} = -2.303\, RT\, pK_a \tag{3}$$

where $\Delta_R G_{AT}$ is the free energy of the acid–base reaction at one anion-termination. Combining Eqs. (2) and (3) gives

$$\Delta_R G_{AT} = -2.303\, RT\, 19.8(\Delta s - 0.20x) \tag{4}$$

where x is the bond-valence contributions of weak hydrogen bonds to the O-atom, showing that the higher the residual valence at an O-atom, the stronger the basicity of the anion termination, the stronger its affinity for hydrogen bonds or O–H bonds, and the more negative the free energy $\Delta_R G_{AT}$ of the corresponding acid–base reaction [31].

Each polyhedron chain at an edge on the surface of a mineral has a series of anion terminations exposed to an ambient aqueous solution, and the aggregate of these anion terminations controls the reactivity of the atoms at the exposed edge. The residual valence of an edge may be defined as the mean residual valence on anion terminations (along its translation length) [31]. Different polyhedron chains have different types of anion termination, each of which has a specific pK_a, Lewis basicity and $\Delta_R G_{AT}$ value for a corresponding acid–base reaction.

Consider a polyhedron chain with b and c different types of anion termination along its repeat length. The pK_a value of an acid–base reaction involving this

polyhedron chain, ΔpK_{PC}, is a function of the types and numbers of different anion-terminations along the chain, and may be written as $\sum \Delta pK_{PC}$, i.e., the sum of the pK_a values of acid–base reactions at the corresponding anion-terminations:

$$\sum \Delta pK_{PC} = [b \times pK_{a1} + c \times pK_{a2}]/(b + c) \quad (5)$$

$$\sum \Delta pK_{PC} = [b \times \Delta s_1 + c \times \Delta s_2]/(b + c) \quad (6)$$

The right-hand side of Eq. (6) is the O-atom residual valence for a polyhedron chain and correlates with the average pK_a-value and the free energy of the acid–base reactions along a polyhedron chain, indicating the affinity of the constituent O-atoms for hydrogen bonds or O–H bonds [31].

4.2 *Point of Zero Charge and Net Proton Charge: A Bond-Valence Perspective*

The point of zero charge is the point where the total net surface charge is zero [33]. The total net surface charge involves (1) the permanent structural charge caused by isomorphic substitution(s); (2) the net proton charge (i.e., the charge due to binding of H or OH at the surface); (3) the charge of the inner-sphere-complex; (4) the charge of the outer-sphere-complex. An inner-sphere complex occurs where a cation or anion in solution bonds directly to terminations on the surface, whereas an outer-sphere complex occurs if a cation or anion in the solution bonds via (H_2O) groups to terminations on the surface; both types of complex change the net proton charge of the surface. We may simplify this issue from a bond-valence perspective by factoring inner- and outer-sphere complexes into two components: (1) surface ions and (2) aqueous complexes in solution, i.e., we treat inner- and outer-sphere complexes as part of the aqueous solution, considering only the difference in interaction between edges with different net proton charge and the aqueous solution. The net proton charge may be considered as the difference between the incident and exident bond-valences between the terminations at the surface and the species in aqueous solution. A termination that accepts bonds is a *Lewis base* and a termination that donates bonds is a *Lewis acid* [31]. At zero net proton charge, the net strength of the Lewis bases and Lewis acids is zero. Where a surface has zero net proton charge, the pH of the coexisting solution is called the *point of zero net proton charge*, which we will designate as the *point of zero charge*. Weak Lewis bases and Lewis acids occur on a surface at the point of zero charge, and (depending on the intrinsic acidity constant of the acid–base reaction), strong Lewis bases and Lewis acids occur at pH values that differ considerably from the point of zero charge. Thus we may define the point of zero charge of a surface from a bond-valence perspective: *At the point of zero charge of a surface, there is a minimum in the number of strong Lewis acids and Lewis bases (i.e., highly charged terminations) on*

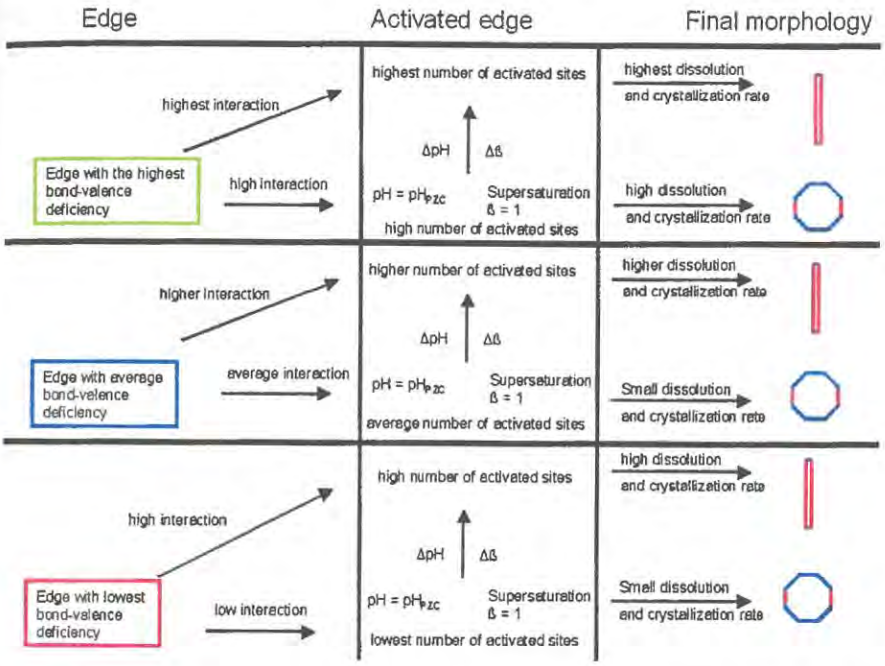

Fig. 4 Summary of the relations between an edge, the corresponding activated edge and the type of crystallization or dissolution. The left column gives the possible types of edges with low, average, and high residual valence, respectively. The central column indicates schematically the increase in activated sites with (**a**) the initial residual valence of an edge, (**b**) ΔpH, the difference between the pH of the solution and the pH_{pzc} of the edge, and (**c**) $\Delta\beta$, the difference between the supersaturation, β, of a solution and the supersaturation at equilibrium (where $\beta = 1$). Increasing ΔpH and $\Delta\beta$ is indicated by an *arrow*. The right column lists the corresponding rates of crystal growth and dissolution, and the final morphologies of a theoretical (0 0 1) face; from [31]

the surface, which results in low bond-valence transfer between surface acceptors and donators, and aqueous species. Thus the lowest interaction between a face and the ambient aqueous solution occurs where the pH of the solution is equal to the point of zero charge of that face, and hence the crystal has very low growth and dissolution perpendicular to that face. The possible types of edges, ambient conditions, and growth rates of faces of different type are summarized in Fig. 4.

5 Application to Minerals

Schindler and Hawthorne [34] and Hawthorne and Schindler [3] showed that many structural and chemical aspects of the uranyl-oxysalt minerals may be understood in terms of bond-valence theory, and Schindler et al. [31, 35] applied the ideas

outlined above to understand aspects of the surface morphology of uranyl-oxysalt minerals. We will review this work and also apply these ideas to hydroxy-hydrated borate minerals.

5.1 Uranyl Minerals

The crystal structures of uranyl minerals are dominated by the structure of the complex uranyl cation: $(UO_2)^{2+}$. The central U^{6+} is coordinated by two O^{2-} anions that form an approximately linear O^{2-}–U^{6+}–O^{2-} group with U^{6+}–O^{2-} bond-valences of ~1.6–2.0 v.u., and the coordination of this complex cation is completed by four to six equatorial anions which receive bond valences of ~0.30–0.70 v.u. The bond-valence requirements of the equatorial anions are most easily satisfied by polymerization of the uranyl polyhedra in the plane of the equatorial anions, φ (=O, OH), and hence the structures of these minerals are dominated by sheets of edge-sharing uranyl polyhedra that are linked in the third dimension by weak alkali-metal–oxygen bonds and hydrogen bonds.

5.1.1 Polyhedron Chains

The $[(UO_2)_8O_2(OH)_{12}]$ sheet is a characteristic structural unit in uranyl minerals and occurs in the crystal structures of schoepite, $[(UO_2)_8O_2(OH)_{12}](H_2O)_{12}$ [36, 37], and fourmarierite, $Pb_2^{2+}[(UO_2)_8O_6(OH)_8](H_2O)_8$ [38]. The sheets are linked by weak Pb–O and/or hydrogen bonds, and the former mineral is of interest as the primary phase formed by alteration of nuclear-fuel rods by aqueous solution. A view of the $[(UO_2)_8O_2(OH)_{12}]$ sheet is shown in Fig. 5, together with the linear polyhedron chains parallel to [1 0 0], [0 1 0], [1 2 0], [2 1 0], and [1 1 0] in the plane of the sheet. The apical uranyl O-atoms project outward from the (0 0 1) surface and determine the reactivity of the (0 0 1) surface itself. These O-atoms receive an average of 1.6–1.7 v.u. from the central U^{6+} cation and can accept only bonds of less than 0.3–0.4 v.u. Hence the uranyl O-atoms can accept only hydrogen bonds and weak bonds from alkali or alkaline-earth cations; they cannot be protonated and are not involved in acid–base reactions at the surface. The situation is very different for surface features such as terraces or steps, as here the equatorial O-atoms in the polyhedron sheet are exposed at the surface. Within the sheet, these equatorial O-atoms bond to two or three U^{6+}-atoms (Fig. 5) and their incident individual bond-valences vary between approximately 0.2 and 0.8 v.u. Where exposed at terraces or edges, these equatorial O-atoms deviate significantly from the valence-sum rule and can protonate and deprotonate in acid–base reactions with the adjacent aqueous solution. Thus edges and terraces are much more reactive than the basal surface, as is the case in dissolution of phyllosilicates which is controlled by acid–base reactions on the corresponding edges (e.g., [39]).

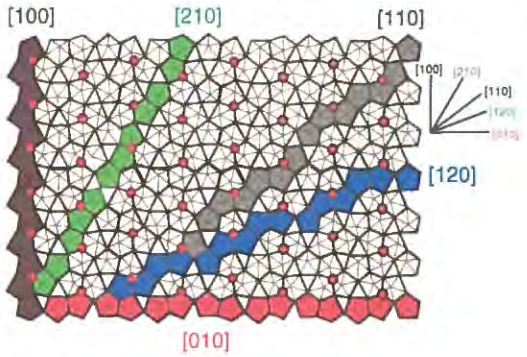

Fig. 5 Polyhedron representation of the uranyl-oxide hydroxy-hydrate sheet in schoepite, $[(UO_2)_8O_2(OH)_{12}](H_2O)_{12}$, showing polyhedron chains parallel to [1 0 0], [0 1 0], [1 2 0], [1 1 0] and [2 1 0], respectively; equatorial O^{2-} anions of the uranyl-polyhedra are shown as *orange/gray circles*, equatorial edges are shown as *heavy black lines*; from [31]

5.1.2 Calculation of pK_a and Lewis Basicity for Different U–O Anion-Terminations

Average equatorial U–φ bond-valences for [6]-, [7]- and [8]-coordinated U^{6+} are 0.64, 0.54, and 0.45 v.u., respectively ([25], calculated with the parameters of [40]). Individual equatorial $^{[a]}$U–φ bond-valences vary over a larger range; for example, the $^{[7]}$U–φ bond-valences in schoepite vary between 0.27 and 0.73 v.u. [36], giving rise to a range of intrinsic acidity constants for one type of anion termination. The types of anion termination in uranyl minerals are limited by the occurrence of [6]-, [7]- and [8]-coordinated U^{6+}: e.g., [6]- and [8]-coordinated U^{6+} never occur together, and always occur with [7]-coordinated U^{6+}. The conformation of an anion termination can be denoted by the symbol $^{[a]}$U–φ–$n^{[b]}$U, where φ is an anion that bonds to one U atom in [*a*]-coordination and *n* U atoms in [*b*]-coordination. In uranyl-oxide minerals, the anion terminations that can occur on edges are as follows: $^{[8]}$U–φ, $^{[7]}$U–φ, $^{[6]}$U–φ, $^{[8]}$U–φ–$^{[8]}$U, $^{[8]}$U–φ–$^{[7]}$U, $^{[7]}$U–φ–$^{[7]}$U, $^{[7]}$U–φ–$^{[6]}$U, $^{[8]}$U–φ–2$^{[7]}$U, $^{[7]}$U–φ–2$^{[7]}$U, and $^{[6]}$U–φ–2$^{[7]}$U (Table 1). The Lewis base-strength of an anion termination is the bond valence required by the termination (to satisfy the valence-sum rule) divided by the number of bonds accepted by the anions of that termination. Thus for the anion-termination $^{[7]}$U–(OH), the bond-valence required is $2 - (0.54 + 0.80) = 0.66$ v.u., the number of bonds required by the anion (assuming a coordination number of [4]) is $4 - 2 = 2$, and the resultant Lewis basicity is $0.66/2 = 0.33$ v.u. For the anion termination $^{[a]}$U–(H_2O), the constituent O-atom has an incident bond-valence sum greater than 2 v.u. and is actually a Lewis acid rather than a Lewis base. The (H_2O) group transforms the bond-valence (*v* v.u.) of the $^{[a]}$U–O bond into two weaker hydrogen bonds of bond-valence *v*/2 [41, 42] and the Lewis acidity of the termination $^{[7]}$U–(H_2O) is $0.54/2 = 0.27$ v.u. Lewis basicities and Lewis acidities of the above anion terminations are given in Table 1.

Table 1 Intrinsic acidity constants, Lewis acidities, and Lewis basicities of equatorial anions terminating the edges on uranyl-sheet minerals

Code	Acids and bases of the anion-termination	pK_{a1}	pK_{a2}	pK_{a3}	Lewis acidity (v.u.)	Lewis basicity (v.u.)
$^{[8]}U$–φ	$^{[8]}U$–$OH_3 \leftrightarrow {}^{[8]}U$–$OH_2^a \leftrightarrow {}^{[8]}U$–$OH^b \leftrightarrow {}^{[8]}U$–$O^c$	−5	6.9	18.8	+0.225[a]	−0.375[b], −0.52[c]
$^{[7]}U$–φ	$^{[7]}U$–$OH_3 \leftrightarrow {}^{[7]}U$–$OH_2^a \leftrightarrow {}^{[7]}U$–$OH^b \leftrightarrow {}^{[7]}U$–$O^c$	−6.7	5.1	17	+0.27[a]	−0.33[b], −0.49[c]
$^{[6]}U$–φ	$^{[6]}U$–$OH_3 \leftrightarrow {}^{[6]}U$–$OH_2^a \leftrightarrow {}^{[6]}U$–$OH^b \leftrightarrow {}^{[6]}U$–$O^c$	−8.7	3.1	15	+0.32[a]	−0.27[b], −0.45[c]
$^{[8]}U$–φ–$^{[8]}U$	$^{[8]}U$–OH_2–$^{[8]}U \leftrightarrow {}^{[8]}U$–OH–$^{[8]}U^a \leftrightarrow {}^{[8]}U$–O–$^{[8]}U^b$	2	13.8			−0.30[a], −0.55[b]
$^{[8]}U$–φ–$^{[7]}U$	$^{[8]}U$–OH_2–$^{[7]}U \leftrightarrow {}^{[8]}U$–OH–$^{[7]}U^a \leftrightarrow {}^{[8]}U$–O–$^{[7]}U^b$	0.2	12			−0.21[a], −0.51[b]
$^{[7]}U$–φ–$^{[7]}U$	$^{[7]}U$–OH_2–$^{[7]}U \leftrightarrow {}^{[7]}U$–OH–$^{[7]}U^a \leftrightarrow {}^{[7]}U$–O–$^{[7]}U^b$	−1.6	10.3			−0.12[a], −0.46[b]
$^{[7]}U$–φ–$^{[6]}U$	$^{[7]}U$–OH_2–$^{[6]}U \leftrightarrow {}^{[7]}U$–OH–$^{[6]}U^a \leftrightarrow {}^{[7]}U$–O–$^{[6]}U^b$	−3.5	8.3			−0.02[a], −0.41[b]
$^{[8]}U$–φ–$2^{[7]}U$	$^{[8]}U$–OH–$2^{[7]}U \leftrightarrow {}^{[8]}U$–O–$2^{[7]}U^a$	5.3				−0.47[a]
$^{[7]}U$–φ–$2^{[7]}U$	$^{[7]}U$–OH–$2^{[7]}U \leftrightarrow {}^{[7]}U$–O–$2^{[7]}U^a$	3.5				−0.38[a]
$^{[6]}U$–φ–$2^{[7]}U$	$^{[6]}U$–OH–$2^{[7]}U \leftrightarrow {}^{[6]}U$–O–$2^{[7]}U^a$	2.5				−0.28[a]

The superscripts a, b, and c denote the Lewis acidities and Lewis basicities and their corresponding terminations

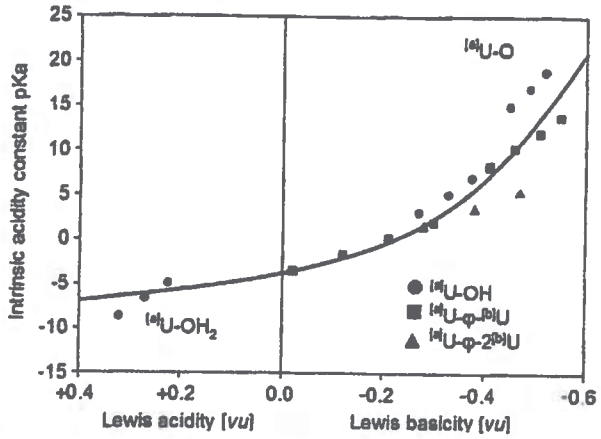

Fig. 6 Lewis basicity as a function of intrinsic acidity constant, pK_a, of anion terminations on the edges of uranyl sheets; from [31]

On the (0 0 1) face of schoepite, there are three different equatorial-anion terminations: $^{[7]}U–(OH)–2^{[7]}U$, $^{[7]}U–(OH)–^{[7]}U$, and $^{[7]}U–O–^{[7]}U$. The characteristic bond-valence for the equatorial $^{[7]}U–\varphi$ bond in schoepite is 0.47 v.u., and as discussed above, we use a coordination number of [4] for O at the surface of the mineral. The acid–base reactions and pK_a values are

$$[1].\ {}^{[7]}U-(OH)-2^{[7]}U \leftrightarrow {}^{[7]}U-O-2^{[7]}U+H^+ \qquad pK_a = 7.7$$
$$[2].\ {}^{[7]}U-(OH)-{}^{[7]}U \leftrightarrow {}^{[7]}U-O-{}^{[7]}U+H^+ \qquad pK_a = 13.1$$
$$[3].\ {}^{[7]}U-(OH_2)-{}^{[7]}U \leftrightarrow {}^{[7]}U-(OH)-{}^{[7]}U+H^+ \qquad pK_a = 1.2$$

The pK_a value is calculated using the mean incident bond-valence at O in the anion termination on the LHS of each reaction. Thus in [1], the O atom receives $0.47 \times 3 + 0.20$ (from a hydrogen bond) which equals 1.61 v.u. Using this value in Eq. (1) gives $pK_a = -19.8(1.61 - 2) = 7.7$. The values in [2] and [3] were calculated in the same way. It should be noted that the calculated pK_a-value of 7.7 for Eq. (1) is in good agreement with an experimentally determined pK_a-value of ~7, which was extrapolated on the basis of titrations of dehydrated schoepite in NaCl solutions of different concentration [31]. The correlation between pK_a and the Lewis basicities and Lewis acidities of the terminations of Table 1 is shown in Fig. 6. These values were calculated with characteristic bond-valences for $^{[6]}U–O$, $^{[7]}U–O$, and $^{[8]}U–O$ given in [25]. The values in Table 1 indicate the correlation between the acid- and base-strengths of an anion termination and the magnitude of the residual valence on its anion terminations. Exact pK_a-values for anion-terminations on the basal surfaces of any uranyl mineral must be calculated using the average U–O bond-valence in the corresponding structure (as shown above for the basal surface of schoepite).

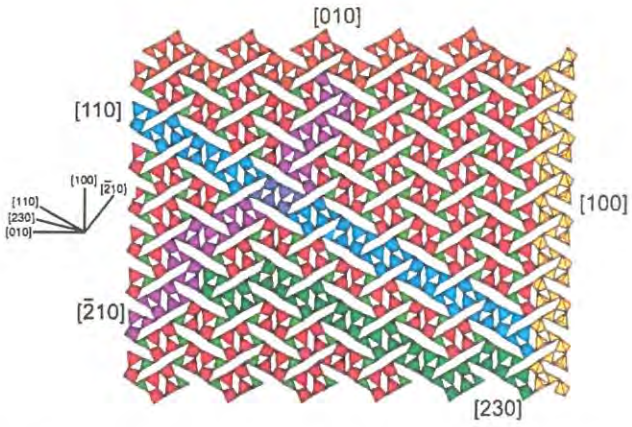

Fig. 7 Polyhedron representation of the borate sheet in fabianite, $Ca_2[B_6O_{10}(OH)_2]$; polyhedron chains are shown parallel to [1 0 0], [0 1 0], [1 1 0], [1 2 0], and [2 3 0], respectively, the directions of which are indicated by the *labeled lines*

5.2 *Borate Minerals*

The crystal structures of borate minerals are dominated by the presence of both ($B\varphi_3$) triangles and ($B\varphi_4$) tetrahedra with B–O bond-valences of ~1.00 and 0.75 v.u., respectively. The valence-sum rule allows polymerization of these two groups and they form structures with isolated polyhedra, clusters, chains, sheets, and frameworks of ($B\varphi_3$) triangles and ($B\varphi_4$) tetrahedral [18, 43, 44].

5.2.1 Polyhedron Chains

The crystal structure of fabianite, $Ca_2[B_6O_{10}(OH)_2]$ [45], consists of sheets of composition $[B_6O_{10}(OH)_2]$, parallel to (0 0 1) and linked in the third dimension by Ca. Two ($B\varphi_4$) tetrahedra each share a corner with a ($B\varphi_3$) triangle to form a three-membered ring that is very common in borate structures. Two rings share two corners between ($B\varphi_4$) tetrahedra to form a $[B_6\varphi_{14}]$ group, and these groups share corners to form a $[B_6\varphi_{12}]$ sheet. Figure 7 shows a view of this sheet, together with the polyhedron chains parallel to [1 0 0], [0 1 0], [1 1 0], [2 1 0], and [2 3 0] in the plane of the sheet. The situation with regard to anion terminations is more complicated than in the case of uranyl-oxide minerals. Figure 8 shows the [0 1 0] polyhedron chain on the (0 0 1) surface (cf. Fig. 3) with the incident bond-valence required by the surface anions for adherence to the valence-sum rule. Most anions require an incident hydrogen bond for adherence to the valence-sum rule, and only a small number of surface anions are (OH) groups (and hence available for (de-) protonation reactions with aqueous species in solution). Figure 9 shows the edge of a [0 1 0] polyhedron chain on the (0 0 1) surface (cf. Fig. 3), again with the

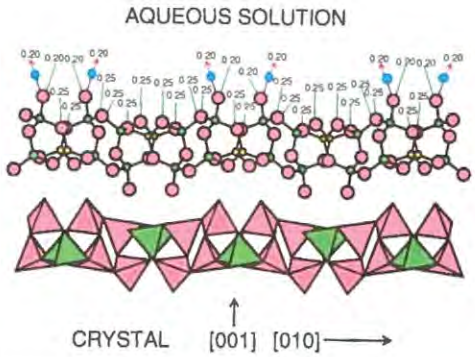

Fig. 8 Polyhedron and ball-and-stick representations of the [0 1 0] polyhedron chain exposed at the (0 0 1) surface in fabianite. The bonds (and corresponding bond-valences required) involving surface anions and constituents of the aqueous solution are shown as *lines* [bond valence donated from the (aquated) cations of the aqueous solution] and as *arrows* (bond valence donated from H atoms of protonated surface anions to anions of the aqueous solution). Note that there are not many protonated anions that can participate in redox reactions with the aqueous solution

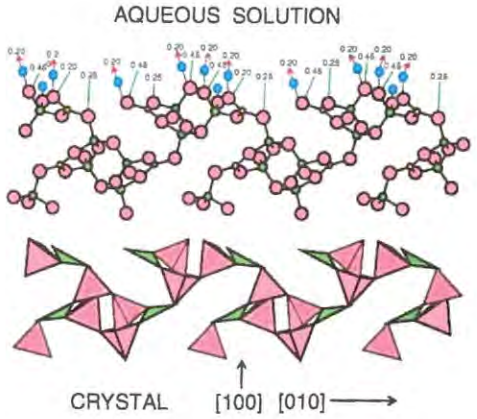

Fig. 9 Polyhedron and ball-and-stick representations of the [0 1 0] polyhedron chain exposed at a (1 0 0) edge on the (0 0 1) surface in fabianite. The bonds (and corresponding bond-valence required) involving surface anions and constituents of the aqueous solution are shown as *lines* (bond valence donated from the aqueous solution) and as *arrows* (bond valence donated from H atoms of protonated surface anions). Note that most of the anions exposed on the edge are protonated and hence can participate in redox reactions with the aqueous solution

incident bond-valence required by the surface anions for adherence to the valence-sum rule. Many anions are now protonated for adherence to the valence-sum rule and hence are available for (de-)protonation reactions with aqueous species in solution. Thus edges (and terraces) exposed on the surface of fabianite are far more reactive, i.e., can act as a nucleus for crystallization or dissolution, than the surface itself.

5.2.2 Lewis Basicity and Acid Strength for Different B–O Anion-Terminations

Average B–φ bond-valences for [3]- and [4]-coordinated B are 1.00 and 0.75 v.u., respectively, and individual B–O bond-valences vary in the ranges 0.86–1.19 v.u. for [3]-coordination and 0.69–0.95 v.u. for [4]-coordination [18]. The valence-sum rule allows all combinations of polymerization between $^{[3]}$B and $^{[4]}$B, and the conformation of an anion termination can be denoted by the symbol $^{[a]}$B–φ–$n^{[b]}$B, where φ is an anion that bonds to one B atom in [*a*]-coordination and *n* B atoms in [*b*]-coordination. In borate minerals, the anion terminations can occur on edges are as follows: $^{[3]}$B–φ, $^{[4]}$B–φ, $^{[3]}$B–φ–$^{[3]}$B, $^{[3]}$B–φ–$^{[4]}$B, $^{[4]}$B–φ–$^{[4]}$B, and $^{[4]}$B–φ–$2^{[4]}$B.

On the [0 1 0] chain on the (0 0 1) face of fabianite, there are three different anion terminations: $^{[4]}$B–φ, $^{[3]}$B–φ–$^{[4]}$B, and $^{[4]}$B–φ–$^{[4]}$B. On the edge of the [0 1 0] chain on the (0 0 1) face of fabianite, there are three different anion terminations on the (0 1 0) chain: $^{[3]}$B–φ, $^{[4]}$B–φ, and $^{[3]}$B–φ–$^{[4]}$B that are involved in acid–base reactions. Oxygen-atoms on the $^{[3]}$B–φ, $^{[4]}$B–φ terminations are highly undersaturated and are most likely protonated ($^{[3]}$B–OH, $^{[3]}$B–OH_2, $^{[4]}$B–OH, $^{[4]}$B–OH_2) in natural waters with pH <12. There is also the possibility that acid–base reactions on the surface of borate minerals involve a change in coordination number of these types of terminations as is observed in aqueous solution: $B(OH)_3^0 + H_2O \leftrightarrow B(OH)_4^- + H^+$, $pK_a = 9.15$. However, changes in coordination number may occur only at kink sites in polyhedron chains, where there is a higher degree of freedom to allow structural change associated with a transformation of a triangle into a tetrahedron or vice versa (i.e., breaking of bonds and rotation of the polyhedron).

6 Crystallization and Dissolution

For minerals crystallizing from low-temperature aqueous solutions, the primary controls on their stability should be (a) the activity of the species in solution and (b) protonation reactions between solid and solution at the edges of polyhedron chains: deprotonation of edge anions promotes attachment of aqueous cation species (i.e., crystallization), whereas protonation of edge anions weakens their bonds to the bulk structure and promotes dissolution. With regard to crystallization, the character and activity of the aqueous species is of interest as these provide groups of atoms that may attach to the solid during crystallization.

6.1 Uranyl Minerals

We have seen that the uranyl cation, $(U^{6+}O_2)^{2+}$, occurs as monomers, dimers, and trimers in aqueous solution. We also discussed that well-crystallized schoepite with

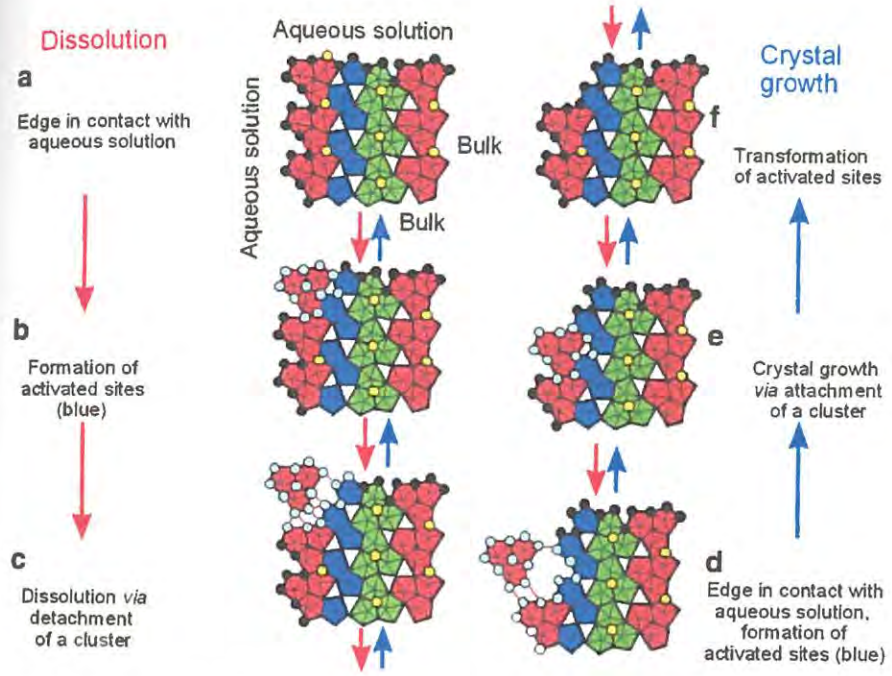

Fig. 10 A schematic of dissolution and growth mechanisms at an edge of a schoepite sheet. The sequence of dissolution is indicated with *downward-directed arrows* and the sequence of crystal growth by *upward-directed arrows*. The schoepite sheet is built of clusters of three (*red/dark-gray* and *green/pale-gray*) and two (*blue/dark-gray*) pentagonal bipyramids which are structurally identical to the principal aqueous species $[(UO_2)_3(OH)_5(H_2O)_5]^+$ and $[(UO_2)_2(OH)_2(H_2O)_6]^{2+}$ in weak acidic solutions (Fig. 4); O^{2-} ligands in the sheet are indicated as *circles*, and ligands which have interacted with the aqueous solutions are indicated in *light blue/white*; (**a**, **f**) activated sites occur only on anion terminations, and activated sites in the layer are transformed to sites; (**b**, **e**) formation of activated sites during dissolution via detachment of a cluster; ligands adjacent to potential detached clusters interact with the solution and are highlighted as *light-blue/white circles*; attachment of a cluster at a kink site occurs via release of one (H_2O) per common ligand between cluster and kink site; (**c**, **d**) breaking (formation) of the U–φ–U bonds and detachment (or approach) of a cluster from (to) an activated kink site on a schoepite layer; from [31]

sheets composed of edge-sharing trimers and dimers of $((U^{6+}O_2)^{2+}\varphi_5)$ polyhedra can be synthesized in a pH range where the trimer $(UO_2)_3(OH_5)^+$ predominates (e.g., [17, 46]). In this regard, Schindler et al. [31] proposed a model for dissolution and crystallization of schoepite that involves the attachment and detachment of trimers, as illustrated in Fig. 10.

Dissolution requires breaking of U–φ–U bonds and subsequent detachment of clusters. The U–φ bonds holding the cluster to the crystal (Fig. 10a) weaken through interaction between the ligands and the adjacent aqueous solution (Fig. 10b), producing what Schindler et al. [31] called an *activated site*, where bonds between ions at activated sites and aqueous species catalyze dissolution or crystal growth at

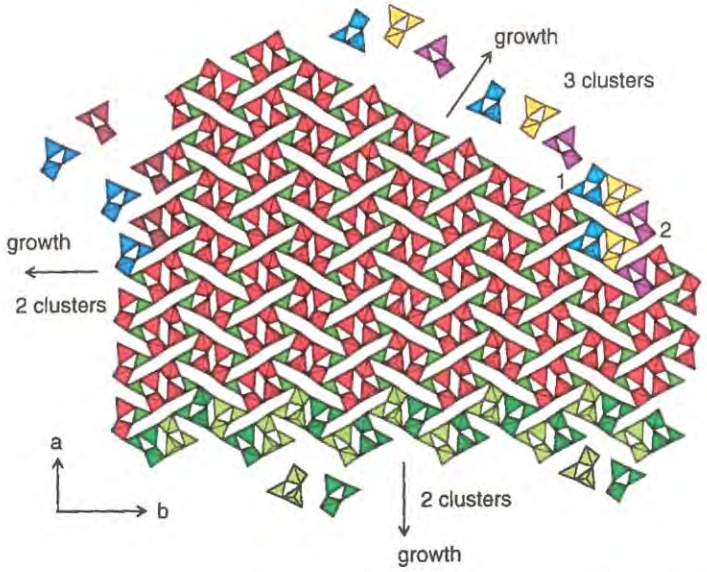

Fig. 11 Schematic of growth at the edges of the (0 0 1) face of fabianite. Growth or dissolution may proceed by attachment or removal of the $[B_3O_3(OH)_5]^{2-}$ cluster that is a major species in aqueous borate solutions

an edge. Here, the U–φ bonds break and the cluster detaches from the crystal, is protonated, and forms an aqueous species (Fig. 10c). Thus an activated site participating in dissolution involves the terminations around a polyhedron cluster where protonation or strong bonds between ligands and aqueous species result in weakening of U–φ bonds.

Crystallization occurs via attachment of clusters at activated sites at anion terminations on the edge of polyhedron chains. Attachment produces one additional (H_2O) or (OH) group per common corner between cluster and anion termination (Figs. 10d,e). Thus at an activated site involved in crystal growth, there are strong hydrogen bonds from anion terminations to a polyhedron cluster in solution. The other anions of the cluster and the (former) activated site stay activated until the anions do not require additional bond-valence from aqueous species (Fig. 10f).

6.2 *Borate Minerals*

As mentioned above, the species in aqueous borate solutions can also be seen embedded in all borate structures, suggesting that crystallization proceeds by condensation of these species to form the solid. This process is illustrated for the structure of fabianite in Fig. 11. The cluster $[B_3O_3(OH)_5]^{2-}$, which shows maximum stability in aqueous solution at a pH of ~9.4 (Fig. 1), consists of a ring of one

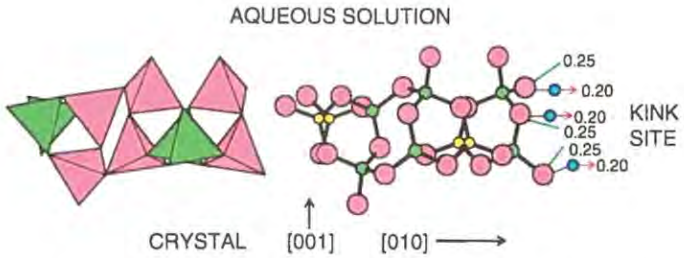

Fig. 12 Polyhedron and ball-and-stick representations of the [1 0 0] polyhedron chain exposed at the (0 0 1) surface in fabianite (as in Fig. 8) but with the polyhedron chain terminated by a kink site. The bonds (and corresponding bond-valence required) involving kink-site anions and constituents of the aqueous solution are shown by *lines* (bond valence donated from the aqueous solution) and *arrows* (bond valence donated from H atoms of protonated surface anions). Note that there are more protonated anions (that can participate in redox reactions with the aqueous solution) at the kink site that there are exposed to the aqueous solution on the (0 0 1) surface (Fig. 7)

($B\varphi_3$) group and two ($B\varphi_4$) groups that is the fundamental building block of the fabianite structure. As indicated in Fig. 11, growth can proceed in any direction on the surface by condensation of $[B_3O_3(OH)_5]^{2-}$ groups in various combinations.

7 Quantitative Aspects of Crystallization and Dissolution

So far, we have put a qualitative mechanism in place for crystallization and dissolution. Now we will make this mechanism more quantitative.

7.1 Residual Valence, Kink Sites, and O^{2-} Ligands

Above, we have considered edges (and terraces) in terms of continuous polyhedron chains. However, during growth, such polyhedron chains will not be continuous. A polyhedron chain forming an edge will terminate at one (or more) place where the atoms of the chain have not yet attached themselves, forming a kink site (Fig. 3). At a kink site, the edge anions are protonated and form an activated site (Fig. 12). Hence the residual valence of an edge increases with its number of kink sites. A larger number of kink sites on an edge (i.e., a high residual valence) favors attachment of polyhedra from the aqueous solution because an attached polyhedron can share more common ligands with the polyhedra of the existing structure than it can on an edge with less kink sites. Hence one expects a correlation between the residual valence of an edge and the growth rate of that edge. Moreover, the number of activated sites on an edge during dissolution or crystal growth should correlate with the difference between the pH of the solution and the point of zero charge of the edge.

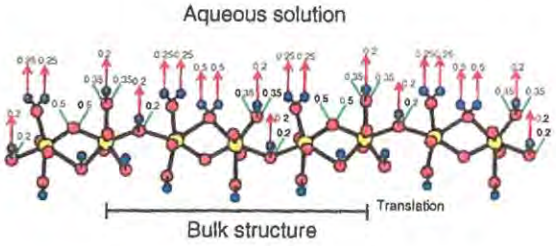

Fig. 13 Ball-and-stick model of a possible activated edge on (0 0 1) parallel to [0 1 0] in schoepite; legend as in Fig. 8; modified from [31]

7.2 Uranyl Minerals

7.2.1 Activated Sites and Edges in Schoepite

Consider a polyhedron chain in schoepite parallel to the [0 1 0] edge (Fig. 5). In the repeat period of the chain, there are one $^{[7]}$U–O–$^{[7]}$U, one $^{[7]}$U–(H_2O)–$^{[7]}$U, two $^{[7]}$U–(OH), two $^{[7]}$U–(H_2O), and two $^{[7]}$U–(OH)–$^{[7]}$U terminations that interact with the aqueous solution (Fig. 13). For arithmetic simplicity, we assign an average bond-valence of 0.50 v.u. to a $^{[7]}$U–φ bond (rather than the grand mean value of 0.47 v.u., see above). The O-atom of a $^{[7]}$U–(H_2O) group receives 0.50 v.u. from $^{[7]}$U and requires an additional 2 × 0.75 v.u. from the two H atoms of the (H_2O) group in order to satisfy the valence-sum rule. Accordingly, each H-atom forms a hydrogen bond of 0.25 v.u. with the aqueous species. The O-atom of a $^{[7]}$U–(OH) group receives 0.50 v.u. from $^{[7]}$U and 0.80 v.u. from the H atom of the (OH) group (which in turn forms a hydrogen bond of 0.20 v.u. with the aqueous species), and the O atom requires a further 0.70 v.u. from cations in solution. The central O–atom of an $^{[7]}$U–(OH)–$^{[7]}$U group receives 2 × 0.50 v.u. from two $^{[7]}$U–O bonds and 0.80 v.u. from the H-atom of the (OH) group and requires an additional 0.20 v.u. from a bond (or bonds) from an aqueous species. The central O-atom of an $^{[7]}$U–O–$^{[7]}$U group requires an additional 1.0 v.u. from bonds involving the aqueous species. The O-atom of a $^{[7]}$U–(H_2O)–$^{[7]}$U group accepts 2 × 0.50 v.u. from two $^{[7]}$U–O bonds and requires an additional 2 × 0.50 v.u. from two O–H bonds; therefore, the $^{[7]}$U–(H_2O) group donates two hydrogen bonds with bond-valence of 0.50 v.u. The acid–base equilibria between the Lewis acids and bases are listed in Table 1. The pK_a values indicate that strong Lewis bases (such as $^{[7]}$U–O–$^{[7]}$U) and Lewis acids (such as $^{[7]}$U–(H_2O)–$^{[7]}$U) occur only at high and low pH, respectively: the number of strong Lewis bases and acids on the [0 1 0] edge is very small in weak acidic, neutral, and weak basic solutions [31].

7.2.2 Left Terminations and Right Terminations

The surface of a crystal grows primarily by attaching species (usually polyhedra) to the dominant edges on that surface. The orientations of these edges are controlled by the orientation of the strongly bonded polyhedron chains on that surface. There are two important factors to be considered here: (1) polyhedron chains that

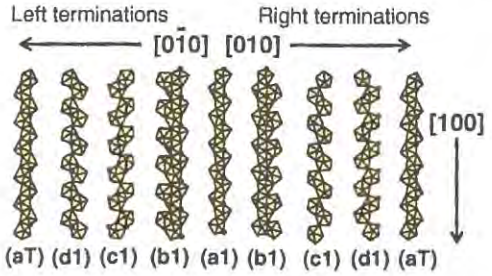

Fig. 14 The left and right chain terminations for different conformations of the polyhedron chain parallel to the [1 0 0] edge in the uranyl sheet of schoepite; the positions of O^{2-} anions are indicated by *circles*. For left terminations, the bulk structure continues to the right, and the surface occurs to the left, and vice versa

are not bilaterally symmetric will expose different atomic arrangements on edges facing in opposite directions, e.g., the (0 1 0) edge of a [1 0 0] chain (as shown in Fig. 14) and the (0 $\bar{1}$ 0) edge of a [1 0 0] chain; thus, the chain shown in the center of Fig. 14 (labeled a1) has different atomic arrangements on the left and right sides (referred to relative to its length), and these we designate as *left terminations* and *right terminations*. (2) As an edge grows by accretion of polyhedra, the atomic arrangement at that edge changes to give a series of arrangements, until the original arrangement occurs again after the accretion of one unit-cell in the direction of growth. When considering the conformation of an edge exposed to an aqueous solution, a series of atomic arrangements must therefore be considered.

This is illustrated in Fig. 14 for chains parallel to [1 0 0] in schoepite. These different terminations are exposed to the left or right of the length of the chain. We designate the different parallel chains as a1, b1, etc. (Fig. 14). There are two $^{[7]}$U–(OH) terminations and four $^{[7]}$U–(OH)–$^{[7]}$U terminations in chain a1. For $^{[7]}U^{6+}$–O = 0.47 and O–H = 0.80 v.u., the O atoms involved in the two $^{[7]}$U–(OH) terminations receive $(2 \times 1 \times 0.47 + 2 \times 0.8) = 2.54$ v.u., and the O atoms involved in the four $^{[7]}$U–(OH)–$^{[7]}$U terminations receive $(4 \times 2 \times 0.47 + 4 \times 0.8) = 6.96$ v.u. The aggregate residual valence of the O atoms involved in the terminations along this chain is $4 - 2.54 + 8 - 6.96 = 2.50$ v.u. Obviously the residual valence along a polyhedron chain is a function of the number of highly charged terminations (e.g., U–(OH): −0.5; U–O–U: −1.0; U–O: −1.5 v.u.).

Figure 15 shows the normalized residual valence of the left- and right-terminations of the chains parallel to [1 0 0], [2 1 0], [1 1 0], [1 2 0] and [0 1 0] in schoepite. Edges involving polyhedron chains with low normalized residual valence will grow slowly, whereas edges involving polyhedron chains with high normalized residual valence will grow rapidly (as high residual valence at anion terminations promotes acid–base reactions with the solution and corresponding crystallization or dissolution). The relative morphology of crystals of schoepite will be controlled in the (1 0 0) plane by the relative magnitudes of the residual valence of polyhedron chains of the form (*h k* 0) (i.e., parallel to the F face): sheets should elongate in the direction of chains with high residual valence and the dominant edges should be controlled by chains with low residual valence. Of the chains shown in Fig. 14, some show major

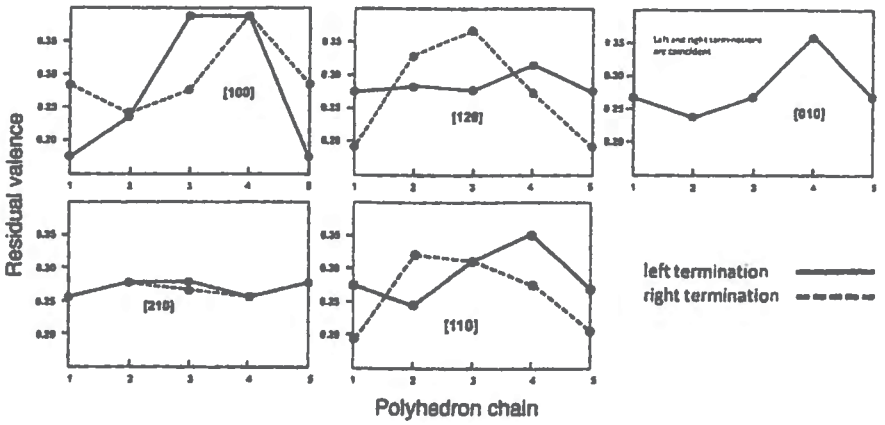

Fig. 15 The calculated residual valence per unit length (v.u./Å) of the polyhedron chains parallel to the [1 0 0], [0 1 0], [1 2 0], [1 1 0], and [2 1 0] edges on the (0 0 1) face for both left and right terminations; the numbers along the abscissa denote the different conformations of each chain, and the corresponding values of the residual valence per repeat are shown on the ordinate

differences in their normalized residual valence with the different types of termination (e.g., the [1 0 0] polyhedron chain), whereas others show little difference with the different types of termination (e.g., the [2 1 0] polyhedron chain). Let us consider the [1 0 0] polyhedron chain. Conformations with high normalized residual valence (e.g., right terminations a3 and a4, Fig. 14) will protonate and deprotonate rapidly in acid–base reactions with the adjacent aqueous solution and change quickly to other conformations. Other conformations with low normalized residual valence (e.g., right terminations a1, a2 and a5, Fig. 14) will protonate and deprotonate far more slowly and the growth rate of the polyhedron chain will be controlled by these conformations with low normalized residual valence. Thus from Fig. 15, we predict the following dominance of edges for the (0 0 1) face of schoepite: [1 0 0] > [1 1 0] ≈ [1 2 0] > [0 1 0] > [2 1 0].

Figure 16a shows the morphology of a crystal of synthetic schoepite grown on the (1 0 4) face of calcite [20, 31]. The edges [1 2 0], [1 0 0], [1 1 0], and [0 1 0] are present (Fig. 16a, right) and [1 2 0] is absent, as predicted above. Figure 16b shows a schoepite crystal from Katanga, Democratic Republic of Congo [47], with a prominent (0 0 1) face slightly elongate along [0 1 0]. The edges defining the (0 0 1) face have indices [1 0 0], [1 1 0], [1 2 0], and [0 1 0] (Fig. 15b, right).

7.3 Borate Minerals

Figures 17a,b show the crystal morphology of nobleite, $Ca[B_6O_9(OH)_2](H_2O)_3$ [48], and tunellite, $Sr[B_6O_9(OH)_2](H_2O)_3$ [49], which contain sheets of polymerized borate polyhedra (Fig. 17c). The morphology of these crystals is defined by

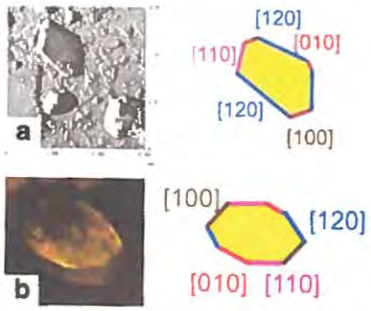

Fig. 16 (**a**) AFM image of a synthetic schoepite crystal grown in a weak acidic solution on the calcite (1 0 4) surface (from [20]), plus a sketch of the crystal which shows the [1 2 0], [1 1 0], [1 0 0], and [0 1 0] edges; (**b**) schoepite crystals (from [47]) plus a sketch of crystal showing a prominent (0 0 1) face that is outlined by the [1 2 0], [1 1 0], [1 0 0], and [0 1 0] edges

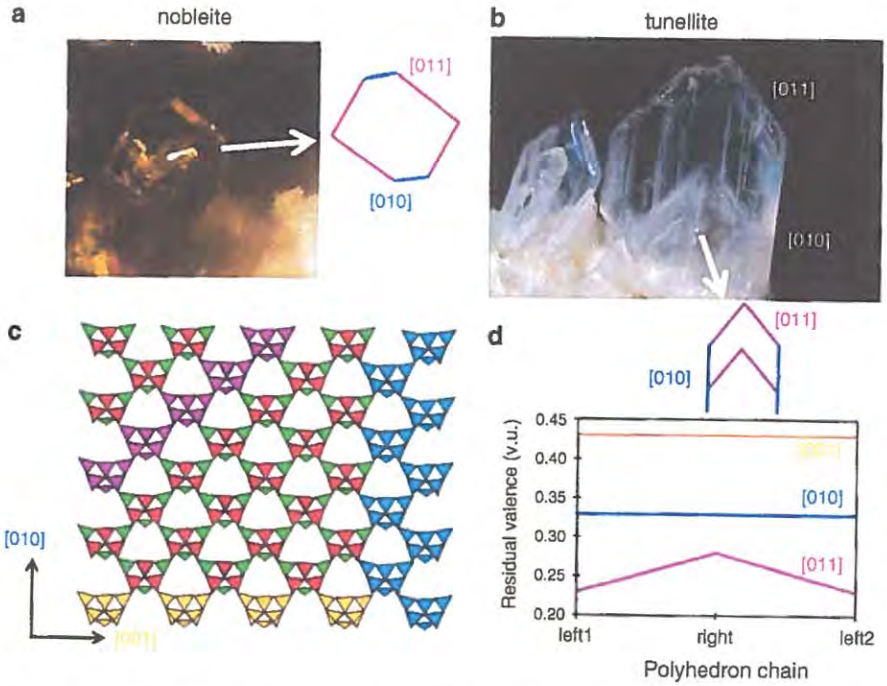

Fig. 17 (**a**, **b**) Photographs of nobleite and tunellite crystals (from [50]); (**c**) sheet of polymerized polyhedra in the structures of nobleite and tunellite; (**d**) sketch of the basal surface of the crystals of nobleite and tunellite and calculated residual valence of the polyhedron chains parallel to the [0 0 1], [0 1 0], and [0 1 1] edges

prominent basal F-faces parallel to the sheets of polymerized polyhedra. The morphology of the F-face itself is defined by edges which are parallel to polyhedron chains within the sheet of polyhedra. Figure 17d shows the normalized residual

valence of the left- and right-terminations of the chains parallel to [1 0 0], [1 1 0] and [0 1 0]. Following the arguments given above (edges involving polyhedron chains with low normalized residual valence will grow slowly, whereas edges involving polyhedron chains with high normalized residual valence will grow rapidly), we predict the following dominance of edges for the (1 0 0) faces of nobleite and tunellite: [0 1 1] > [0 1 0] > [0 0 1]. Figure 17 shows sketches of the morphology of the F-face for crystals of nobleite and tunellite, indicating that their morphologies are in accord with our predictions.

8 Summary

Here, we have integrated many individual aspects of the growth and dissolution of minerals into a coherent description of these processes based on bond-valence theory and apply it to aspects of the morphology of uranyl-oxide hydroxyl hydrate and borate minerals. Below, we summarize the main aspects of this work:

1. In borate and uranyl-oxide hydroxyl-hydrate minerals, structural diversity occurs by polymerization of a small number of clusters (or fundamental building blocks).
2. These minerals crystallize from aqueous or hydrothermal solutions, and the FBBs occur as aqueous species in solution.
3. It seems reasonable that crystallization of these minerals occurs by condensation of the clusters in solution.
4. Periodic bond-chains are strongly related to the occurrence of faces on a crystal (and, in turn, the major growth directions of a crystal) [21–23]. We refer to periodic bond-chains as *polyhedron chains*.
5. Anions at the surface (i.e., exposed to an ambient aqueous solution) are called *terminations*, and the incident residual valence at a termination controls its reactivity (i.e., is the driving force for reaction with the aqueous solution).
6. The residual valence of a polyhedron chain controls the growth or dissolution rate at the crystal face associated with that chain and may be calculated as the net residual valence of the terminations along the repeat length of the polyhedron chain.
7. It is well known that growth and dissolution of individual faces on a crystal are controlled primarily by the occurrence of edges, terraces, and kink sites along those edges and terraces. The terminations associated with these features have much higher residual valence than the terminations on the surface expression of the polyhedron chains, making them much more susceptible to (de-) protonation reactions involving species in aqueous solution (i.e., crystallization or dissolution).
8. The bond-valence of an anion termination on a terminating polyhedron chain correlates with the intrinsic acidity constant, pK_a, and with the free energy, ΔG_{AT}, of the corresponding acid–base reaction.

9. Interaction between the ligands and the adjacent aqueous solution produces *activated sites*, and bonds between ions at activated sites and aqueous species catalyze dissolution or crystal growth at an edge.
10. Crystal growth and dissolution processes on an edge are catalyzed by the activated sites and increase with their number and the strength of the bonds between the corresponding anion terminations and the aqueous species.
11. From a bond-valence perspective, at the point of zero charge of a surface, there is a minimum in the number of strong Lewis acids and Lewis bases (i.e., highly charged terminations) on the surface, which results in low bond-valence transfer between surface acceptors and donators, and aqueous species. Thus the lowest interaction between a face and the ambient aqueous solution occurs where the pH of the solution is equal to the point of zero charge of that face, and hence the crystal has very low growth and dissolution perpendicular to that face.
12. We may calculate the pK_n and Lewis basicity for different anion-terminations, and from this calculate the aggregate residual valence along polyhedron chains. Edges involving polyhedron chains with low normalized residual valence will grow slowly, whereas edges involving polyhedron chains with high normalized residual valence will grow rapidly.
13. The relative morphology of prominent basal faces of crystals will be controlled by the relative magnitudes of the residual valence of polyhedron chains parallel to specific edges. Faces should elongate in the direction of chains with low residual valence and should not be defined by edges parallel to chains with high residual valence.

Acknowledgments FCH was supported by a Canada Research Chair in Crystallography and Mineralogy, and FCH and MS were supported by Discovery Grants from the Natural Sciences and Engineering Research Council of Canada.

References

1. Brown ID (2002) The chemical bond in inorganic chemistry: the bond-valence model. Oxford University Press, Oxford
2. Schindler M, Hawthorne FC (2001) A bond-valence approach to the structure, chemistry and paragenesis of hydroxy-hydrated oxysalt minerals: II. crystal structure and chemical composition of borate minerals. Can Mineral 5:1243–1256
3. Hawthorne FC, Schindler M (2008) Understanding the weakly bonded constituents in oxysalt minerals. Z Kristallogr 223:41–68
4. Hawthorne FC (2012) A bond-topological approach to theoretical mineralogy: crystal structure, chemical composition and chemical reactions. Phys Chem Mineral 39:841–874
5. Hawthorne FC (1979) The crystal structure of morinite. Can Mineral 17:93–102
6. Hawthorne FC (1983) Graphical enumeration of polyhedral clusters. Acta Crystallogr A39:724–736
7. Hawthorne FC (1985) Towards a structural classification of minerals: the $^{VI}M^{IV}T_2O_n$ minerals. Am Mineral 70:455–473

8. Ingri N (1963) Equilibrium studies of polyanions containing B^{III}, Si^{IV}, Ge^{IV} and V^{V}. Svensk Kem Tidskr 75:3–34
9. Janda R, Heller G (1979) Ramanspektroskopische. Untersuchungen an festen und in Wasser gelösten Polyboraten. Z Naturforsch 34b:585–590
10. Salentine CG (1983) High-field boron-11 NMR of alkali borates. Aqueous polyborate equilibria. Inorg Chem 22:3920–3924
11. Müller D, Grimmer AR, Timper U, Heller G, Shakibaie-Moghadam M (1993) ^{11}B-MAS-NMR untersuchungen zur anionenstruktur von boraten. Z Anorg Allg Chem 619:1262–1268
12. Maya L (1976) Identification of polyborate and fluoropolyborate ions in solution by Raman spectroscopy. Inorg Chem 15:2179–2184
13. Janda R, Heller G (1979) B–NMR-spektroskopische. Untersuchungen an wäßrigen Polyboratlösungen. Z Naturforsch 34b:1078–1083
14. Christ CL, Truesdell AH, Erd RC (1967) Borate mineral assemblages in the system Na_2O–CaO–MgO–B_2O_3–H_2O. Geochim Cosmochim Acta 31:313–337
15. Schindler M, Hawthorne FC (2001) A bond-valence approach to the structure, chemistry and paragenesis of hydroxy-hydrated oxysalt minerals: III. paragenesis of borate minerals. Can Mineral 5:1257–1274
16. Grenthe I, Fuger J, Konings RJM, Lemire RJ, Muller AB, Nguyen-Trung C, Wanner H (2004) Chemical thermodynamics of Uranium. Nuclear Energy Agency, OECD Nuclear Energy Agency, Data Bank Issy-les-Moulineaux, France
17. Tsushima S, Rossberg A, Ikeda A, Müller K, Scheinost AC (2007) Stoichiometry and structure of uranyl(VI) hydroxo dimer and trimer complexes in aqueous solution. Inorg Chem 46:10819–10826
18. Hawthorne FC, Burns PC, Grice JD (1996) The crystal chemistry of boron. Rev Mineral 33:41–115
19. Langmuir D (1978) Uranium solution-mineral equilibria at low temperatures with applications to sedimentary ore deposits. Geochim Cosmochim Acta 42:547–569
20. Schindler M, Putnis A (2004) Crystal growth of schoepite on the (104) surface of calcite. Can Mineral 42:1667–1681
21. Hartman P, Perdok WG (1955) On the relations between structure and morphology of crystals I. Acta Crystallogr 8:49–52
22. Hartman P, Perdok WG (1955) On the relations between structure and morphology of crystals II. Acta Crystallogr 8:521–524
23. Hartman P, Perdok WG (1955) On the relations between structure and morphology of crystals II. Acta Crystallogr 8:525–529
24. Hawthorne FC, Krivovichev SV, Burns PC (2000) The crystal chemistry of sulfate minerals. Rev Mineral Geochem 40:1–112
25. Burns PC (1999) The crystal chemistry of uranium. Rev Mineral 38:23–90
26. Krivovichev SV, Filatov SK (1999) Structural principles for minerals and inorganic compounds containing anion-centrered tetrahedra. Am Mineral 84:1099–1106
27. Hiemstra T, Venema O, Van Riemsdijk WH (1996) Intrinsic proton affinity of reactive surface groups of metal (hydr)oxides: the bond valence principle. J Colloid Interface Sci 184:680–692
28. Bickmore BR, Rosso KM, Nagy KL, Cygan RT, Tadanier CJ (2003) Ab initio determination of edge surface structures for dioctahedral 2:1 phyllosilicates: implications for acid–base reactivity. Clays Clay Mineral 51:359–371
29. Bickmore BR, Tadanier CJ, Rosso KM, Monn WD, Eggett DL (2004) Bond-valence methods for pKa prediction: critical reanalysis and a new approach. Geochim Cosmochim Acta 68:2025–2042
30. Schindler M, Hawthorne FC (2001) A bond-valence approach to the structure, chemistry and paragenesis of hydroxy-hydrated oxysalt minerals: I. theory. Can Mineral 5:1225–1242
31. Schindler M, Mutter A, Hawthorne FC, Putnis A (2004) Prediction of crystal morphology of complex uranyl-sheet minerals. I. Theory. Can Mineral 42:1629–1649

32. Faure G (1998) Principles and applications of geochemistry: a comprehensive textbook for geology students. Prentice Hall, Upper Saddle River
33. Stumm W (1992) Chemistry of the solid-water interface. Wiley, New York
34. Schindler M, Hawthorne FC (2004) A bond-valence approach to the uranyl-oxide hydroxy-hydrate minerals: chemical composition and occurrence. Can Mineral 42:1601–1627
35. Schindler M, Mutter A, Hawthorne FC, Putnis A (2004) Prediction of crystal morphology of complex uranyl-sheet minerals. II. Observation. Can Mineral 42:1651–1666
36. Finch RJ, Cooper MA, Hawthorne FC, Ewing RC (1996) The crystal structure of schoepite, $[(UO_2)_8O_2(OH)_{12}](H_2O)_{12}$. Can Mineral 34:1071–1088
37. Finch RJ, Hawthorne FC, Ewing RC (1998) Structural relations among schoepite, metaschoepite and "dehydrated schoepite". Can Mineral 36:831–845
38. Piret P (1985) Structure cristalline de la fourmariérite, $Pb(UO_2)_4O_3(OH)_4{\cdot}4H_2O$. Bull Minéral 108:659–665
39. Rufe E, Hochella M Jr (1999) Quantitative assesment of reactive surface area of phlogopite dissolution during acid dissolution. Sci 285:874–876
40. Burns PC, Ewing RC, Hawthorne FC (1997) The crystal chemistry of hexavalent uranium: polyhedron geometries, bond-valence parameters and polymerization of polyhedra. Can Mineral 35:1551–1570
41. Hawthorne FC (1992) The role of OH and H_2O in oxide and oxysalt minerals. Z Kristallogr 201:183–206
42. Hawthorne FC (1994) Structural aspects of oxides and oxysalt crystals. Acta Crystallogr B50:481–510
43. Burns PC, Grice JD, Hawthorne FC (1995) Borate minerals. I. Polyhedral clusters and fundamental building blocks. Can Mineral 33:1131–1151
44. Grice JD, Burns PC, Hawthorne FC (1999) Borate minerals II. A hierarchy of structures based on the borate fundamental building block. Can Mineral 37:731–762
45. Konnert JA, Clark JR, Christ CL (1970) Crystal structure of fabianite, $CaB_3O_5(OH)$, and a comparison with the structure of its synthetic dimorph. Z Kristallogr 132:241–252
46. Moll H, Reich T, Szabó Z (2000) The hydrolysis of dioxouranium (VI) investigated using EXAFS and ^{17}O-NMR. Radiochim Acta 88:411–415
47. http://www.trinityminerals.com/sm/uranium.shtml
48. Karanovic L, Rosic A, Poleti D (2004) Crystal structure of nobleite, $Ca[B_6O_9(OH)_2]{*}3H_2O$, from Jarandol (Serbia). Eur J Mineral 16:825–833
49. Burns PC, Hawthorne FC (1994) Hydrogen bonding in tunellite. Can Mineral 32:895–902
50. Gerhold G, Kampf AR, Bruland K, Ettensohn D, Behnke D (2006) The photo-atlas of minerals for Windows. Los Angeles county museum of natural history, Gem Mineral Council, Los Angeles